PERGAMON

International Journal of Solids and Structures 40 (2003) 871–879

INTERNATIONAL JOURNAL OF SOLIDS and STRUCTURES

www.elsevier.com/locate/ijsolstr

On the speed of an unconstrained shear band in a perfectly plastic material

T.W. Wright *

US Army Research Laboratory, AMSRL-WM, 4600 Deer Creek Loop, Aberdeen Proving Ground, MD 21005, USA

Received 19 March 2002; received in revised form 18 October 2002

Abstract

It is shown that the speed of an adiabatic shear band may be estimated from its physical and constitutive properties within a constant, which must be obtained from the complete boundary value problem.

Keywords: Adiabatic shear; Plasticity

1. Introduction and background

A subject of considerable interest in the recent literature has been the behavior and characteristics of an adiabatic shear band. Much progress has been made, but one particularly elusive feature has been the speed of propagation of the band. Even the feature whose speed is to be tracked has not been agreed upon completely.

In their study of a shear band, considered as a boundary layer, Gioia and Ortiz (1996) chose to track the forward tip of a contour of constant plastic work as a marker for determining the speed of propagation. Each contour has the form of a long, narrow plume that is widest near the forward tip and narrows significantly at its rear end, which in their study is anchored at the fixed origin of laboratory coordinates. As a simple model they assume that when the plastic work reaches a critical level there is a transition from a stabilizing high value of the work hardening exponent to an unstable low value. Because many materials do seem to experience a saturation of work hardening, this may be a suitable description for some cases. In calculations for the case of impact on the edge of a precracked plate (the Kalthoff problem, see a review by Kalthoff, 2000) they plot the tip speed, U, normalized by the speed of the impactor, V, as a function of the Reynolds number, $\boldsymbol{R} = \rho V^2/S$, and the non-dimensional critical work, $\boldsymbol{W} = w_c/\sigma_0\gamma_0$. Thus, $U/V = f(\boldsymbol{R};\boldsymbol{W})$, where S is a characteristic flow stress, w_c is the critical level of plastic work, and the product $\sigma_0\gamma_0$ represents a characteristic level of plastic work. At constant $\boldsymbol{W}$ the function $f(\cdot)$ rises rapidly for small Reynolds numbers, but becomes nearly constant for values larger than 10 or 12, so that U is approximately

* Tel.: +1-410-306-1943; fax: +1-410-306-0661.
E-mail address: tww@arl.army.mil (T.W. Wright).

PII: S0020-7683(02)00648-0

proportional to V for large Reynolds numbers. The whole curve appears to decrease uniformly for increasing values of critical work. In general, however, there seems to be no way to select the critical level of plastic work a priori, so w_c remains a free parameter. Furthermore, this characterization of the speed of a shear band is tied specifically to the Kalthoff problem and does not appear to be easily generalized to a more complex flow field.

Gioia and Ortiz (1996) also developed solutions for a fully developed shear band, but they did not show how it connects to the forward facing plumes of plastic work or higher temperature.

Another description of a propagating shear band was given by Wright and Walter (1996) for a mode III deformation in a perfectly plastic material. They assumed that the near field around the tip of a fully localized shear band would appear to be steady, as viewed from a coordinate system that translates at a constant speed with the tip. Furthermore, they assumed that all fields would have a similarity form, $r^{\alpha} f(\phi)$, where r is the radius from the moving tip of the band, α is an unknown exponent, and f is an unknown function of the polar angle, ϕ, measured from directly ahead of the band (different alphas and functions for different fields). These assumptions (translation at a constant speed, steady fields as seen from the tip of the band, and a similarity form for the solution) result in a definite set of exponents and a coupled set of ordinary differential equations for the unknown characteristic functions. The radial exponents for particle velocity, stress, and the temperature factor are all small positive numbers so that although there is no singular behavior at the tip, there is rapid variation in the radial coordinate. Furthermore, solution of the equations by standard methods revealed that the particle velocity, which is odd in ϕ, increases rapidly from zero directly ahead of the band, but then makes a transition to nearly constant values that are discontinuous across the shear band where $\phi \to \pm\pi$. Finally, both the flow stress and the temperature show wedges of higher values that open forward from the tip. In addition, the flow stress and the driving traction on the shear band, s_{23}, are continuous to the rear across the fully developed shear band, but s_{23} has a substantially lower value there than it has in the forward ridge. Wright and Walter (1996) also showed that, at least for some simple constitutive models, knowledge of the continuous shear stress and the jump in particle velocity across a fully developed shear band is sufficient information to deduce the complete structure of the band. Thus a transition region between a forward facing wedge and the fully localized shear band to its rear was fully described.

In the original paper, the solution was given in terms of two unknown parameters, namely the speed of the shear band, U, and the initial condition for the temperature function, denoted G_0.

Chen and Batra (1999) using the same approach as Wright and Walter (1996), developed the structure around the tip of a shear band in mode II motion. They found the same exponents for the radial dependence as in mode III, but the angular dependence was much more complicated because in mode II there are two components of velocity, rather than only one, as in mode III. In all other qualitative aspects the two cases are very similar.

At this point it needs to be emphasized that in order to determine the speed of a shear band Gioia and Ortiz (1996) focused their attention on a feature in the forward part of the leading plume of higher flow stress, plastic work, and temperature. In contrast Wright and Walter (1996) and Chen and Batra (1999) focused their attention on the rear of the plume where the transition to a fully developed and fully localized shear band occurs. In the former case, the speed of the shear band was given as a function of two parameters (free field Reynolds number and critical level of plastic work). In the latter cases two parameters were also required, but the speed of the shear band was itself one of those parameters. The other parameter was an initial condition for the similarity ODEs.

Two recent papers, one experimental and the other computational, have shed further light on the question of the speed of a shear band. Guduru et al. (2001) used high-speed optical and infrared observations in a series of Kalthoff experiments on plates made of C300 maraging steel. In this application the optical technique of coherent gradient sensing (CGS) was sensitive to the surface displacement gradient, $\partial u_3/\partial x_2$, in a direction perpendicular to the advancing shear band. The displacement normal to the surface of the plate is u_3, and the surface coordinate perpendicular to the shear band is x_2. Because the impact side of the shear band is in compression parallel to the band and the other side is in relative tension, there is a correspondingly sharp thickening or thinning of the plate on the two sides. As a consequence the CGS technique shows the fully formed shear band with remarkable clarity and permits high-speed observation of the advancing tip at the end of the fully localized region. However, a further consequence is that the material in the shear band actually experiences a mixed mode motion, rather than just mode II, because of the finite thickness of the plate. The somewhat diffuse nature of the tip itself, which is visible in the CGS images and is probably a consequence of the power law behavior in the radial coordinate from the tip, appears to introduce some uncertainty in the precise determination of its position. Nevertheless, the authors have reported five shear band trajectories for five different speeds of the impactor. These trajectories show a certain amount of variation in velocity, including nearly stopping, which may correspond to the arrival of elastic release waves from various boundaries in either the target plate or the impactor. No shear band ever really attains a constant speed, although one seems to come close for part of its trajectory in the results from the fastest impactor striking at 39 m/s. The steady representation should still hold if the velocity is only "slowly varying". The experimental results of Guduru et al. (2001) may lend some support to this point of view. Although the measured speeds of the shear band in the five cases shown are rather variable, the infrared measurements, which were made by an eight by eight array of detectors over a field of view that was 1.1 mm square and placed in the path of the shear band, show the thermal plume extending ahead of the fully developed shear band in qualitative agreement with the computational predictions of Gioia and Ortiz (1996) and also of Needleman and Tvergaard (1995).

Bonnet-LeBouvier et al. (2002) have made a direct computational attack on the problem of the speed of an adiabatic shear band. They consider a strip of material 2.5 mm wide by 200 mm long subjected to equal and opposite driving velocities, $\pm V$, along the long boundaries and periodic boundary conditions on the short boundaries. A defect at one end ensures the formation of a shear band in mode II motion, which may be tracked as it develops. The full balance laws for momentum and energy, including heat conduction, are used. Therefore, the structure of the band and its development are determined by the physics of the problem, not by the mesh used in the calculation. The mesh was carefully graded from very fine to coarse proceeding from the central planes toward the boundary. The authors use linear elasticity and a constitutive law for the plastic flow stress of the form

$$\sigma_e = K(\varepsilon + \varepsilon_0)^n T^{-\nu}(D + D_0)^m, \tag{1}$$

where $\sigma_e = \left(\frac{3}{2}\mathbf{S} : \mathbf{S}\right)^{1/2}$ is the flow stress in an equivalent tension test, ε is the equivalent plastic tensile strain, T is the temperature, and $D = \left(\frac{2}{3}\mathbf{d} : \mathbf{d}\right)^{1/2}$ is the plastic strain rate. The other six parameters, K, ε_0, n, ν, D_0, and m, are constants.

The authors begin their study by identifying a set of non-dimensional physical parameters. Then by extensive parametric calculation, varying one parameter at a time, they deduce the dependence of the ratio U/V as a power law function of the various parameters.

The feature that they select to characterize the speed of a shear band in their calculations is the transition between the fully developed band and the forward facing plume. They find that the steady speed of a shear band in their problem may be characterized by three stages if the speed is greater than a small critical speed, below which no shear band forms. In stage I, disregarding the small critical speed, they find that the speed of the band is proportional to the driving velocity at the boundary,

$$\frac{U}{V} = \alpha \frac{K\beta}{\rho c T_0 m}(-An + B), \tag{2}$$

where T_0 is the initial temperature, and β is the Taylor–Quinney factor, usually taken to lie between about 0.85 and 1.0, which expresses the fraction of plastic work converted to heat. They find that stage II, which is a transition region between stages I and III, cannot be easily characterized. In stage III they find that the speed of the shear band becomes independent of the applied velocity

$$U = \eta \frac{K}{\rho} \sqrt{\frac{\beta}{cT_0 m}} (-A'n + B'). \tag{3}$$

The coefficient η depends upon the temperature exponent, v. In the concluding discussion they remark that "... it is most probable that the shear band speed is controlled by the intensity of thermal softening $\partial\sigma_e/\partial T$ ..." in the region directly ahead of the band.

2. Perfectly plastic materials

For a perfectly plastic material both the stage I and stage III speeds may be deduced theoretically from the steady similarity solutions of Wright and Walter (1996) for antiplane motion or Chen and Batra (1999) for in-plane motion. For example, Eqs. (17) from Wright and Walter (1996) are:

$$\begin{aligned} w &= U\left\{\frac{2m}{1+m}\frac{\rho c}{a\kappa_0}\right\}^{1/(1+m)}\left(\frac{r}{Ub}\right)^{m/(1+m)} W, \\ \dot{\gamma} &= \frac{1}{b}\left\{\frac{2m}{1+m}\frac{\rho c}{a\kappa_0}\right\}^{1/(1+m)}\left(\frac{r}{Ub}\right)^{-1/(1+m)} \Gamma, \\ g &= \frac{\rho U^2}{\kappa_0}\left\{\frac{2m}{1+m}\frac{\rho c}{a\kappa_0}\right\}^{(1-m)/(1+m)}\left(\frac{r}{Ub}\right)^{2m/(1+m)} G, \\ s &= \rho U^2\left\{\frac{2m}{1+m}\frac{\rho c}{a\kappa_0}\right\}^{1/(1+m)}\left(\frac{r}{Ub}\right)^{m/(1+m)} S. \end{aligned} \tag{4}$$

In this case the flow stress and strain rate correspond to an equivalent shear test. Thus, $s = \left(\frac{1}{2}\mathbf{S}:\mathbf{S}\right)^{1/2}$ and $D = (2\mathbf{d}:\mathbf{d})^{1/2}$. The flow law now is $s = \kappa_0 g(\theta)(1 + b|\nabla w|)^m$ where the softening function is $g = 1 - a\theta$. In all applications $b|\nabla w| \gg 1$, so that $(1 + b|\nabla w|)^m \approx (b|\nabla w|)^m$. As stated in Section 1, U is the speed of the shear band. The non-dimensional functions W, Γ, G, S depend only on the polar angle ϕ, measured from the direction of propagation, and satisfy a coupled set of ordinary differential equations in which the strain rate sensitivity, m, is the only parameter. W is odd, and S, G, and Γ are even in ϕ. The out of plane velocity is w, the flow stress is s and $S = G\Gamma^m$. With the scaling shown in (4), to obtain any solution at all it is necessary that $\Gamma(0) = 1$, Wright and Walter (1996). As a consequence, the other two initial values that fix the initial stress and temperature are equal, $S(0) = G(0) = S_0 = O(1)$. The similarity solution is perhaps best understood as the leading term in a local series solution, e.g., $w = r^\alpha[w_0(\phi) + rw_1(\phi) + \frac{1}{2}r^2 w_2(\phi) + \cdots]$ for the velocity, which must be matched to an exterior solution in which the local solution is embedded. Close to the tip of the shear band the leading term will dominate.

Because of the self-similar form we can write $s(0,r)/S(0) = s(\pi - \varepsilon, r)/S(\pi - \varepsilon)$, where ε is a small number, or in obvious notation;

$$s^+/S_0 = s^-/S^-. \tag{5}$$

After eliminating the radial dependence from the last two equations of (4), using the initial conditions, and inverting for U, we have

$$U = \frac{s^+}{\rho}\sqrt{\frac{1+m}{2m}}\sqrt{\frac{a}{g^+ c}}\frac{1}{\sqrt{S_0}}. \tag{6}$$

Now note that for the assumed constitutive function, we have $a/g^+ = -(s_\theta/s)^+$, so that the expression for the speed of a shear band may be written

$$U = \sqrt{\frac{s^+}{\rho}}\sqrt{\frac{-s_\theta^+}{\rho c}}\sqrt{\frac{1+m}{2m}}\frac{1}{\sqrt{S_0}}. \tag{7}$$

Formula (7) depends only on the conditions directly ahead of the shear band, and the distance r is immaterial so long as it is close to the band where the smallest power of r will dominate the solution. The first factor in Eq. (7) has the dimensions of speed, and the others are non-dimensional. Because $\rho c\,\mathrm{d}\theta = \mathrm{d}W_\mathrm{p}$ for adiabatic heating, we can regard ρc as the amount of plastic work per unit volume to raise the temperature one unit, and therefore, the ratio $-s_\theta/\rho c$ is the dimensionless rate of adiabatic softening per unit plastic work. If the Taylor–Quinney factor were to be used, the expression would read $-\beta s_\theta/\rho c$, but for theoretical reasons $\beta = 1$ in a non-work hardening material, see Wright (2002).

Although (7) was derived from a particular flow law, one may speculate that it holds for any non-work hardening material, especially since the conditions ahead of the band are not extreme so that the linear thermal softening and the power law rate hardening will be reasonable approximations.

Furthermore, from the first and last of (4), after eliminating the dependence on r, we have $w/s = W/\rho US$ and since S is even and W is odd in ϕ, we have a formula for the jump of the velocity across the shear band.

$$[w^-] = 2\frac{W^-}{\rho U}\frac{s^+}{S_0} = U\frac{4m}{1+m}\frac{\rho c}{-s_\theta^+}W^- = 2\sqrt{\frac{2m}{1+m}}\sqrt{\frac{s^+c}{-s_\theta^+}}\frac{W^-}{\sqrt{S_0}}. \tag{8}$$

Finally, after dividing Eq. (7) by Eq. (8), we have

$$\frac{U}{[w^-]/2} = \frac{1}{W^-}\frac{1+m}{2m}\frac{-s_\theta^+}{\rho c}. \tag{9}$$

Eqs. (5), (7)–(9) are the principal results. Plots of the non-dimensional velocity, $W(\pi^-;m)$, and driving shear stress, $S_{23}(\pi^-;m)$, on the fully formed band are shown in Figs. 1 and 2 as a function of the strain rate sensitivity. Data were taken from the computations shown in Wright and Walter (1996) for the case $S_0 = G_0 = 1$.

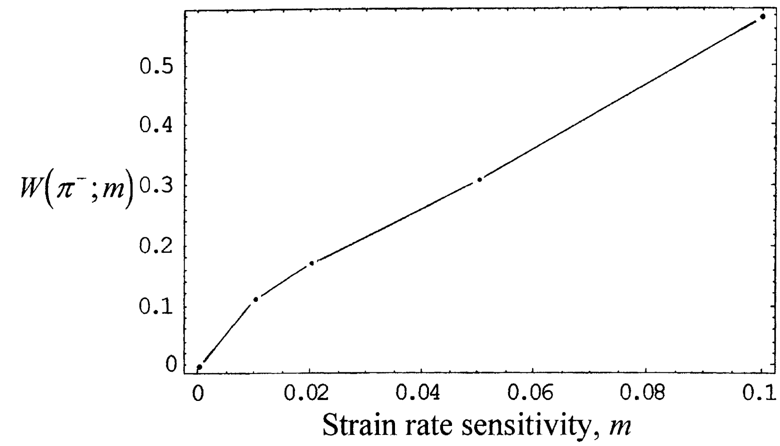

Fig. 1. Plot of the characteristic function for velocity in mode III motion near the shear band as a function of strain rate sensitivity. Data points taken from Wright and Walter (1996).

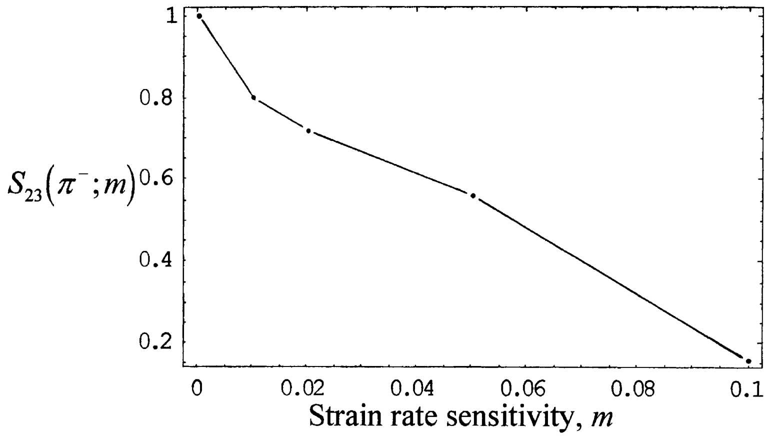

Fig. 2. Plot of the characteristic function for the driving shear stress in mode III motion near the shear band as a function of strain rate sensitivity. Data points taken from Wright and Walter (1996).

In the paper by Chen and Batra (1999) the analysis is similar in spirit, but more complicated in detail because there are two components of velocity. They chose a slightly different scaling for the non-dimensional functions.

$$\begin{aligned}\dot{\gamma} &= \left\{\frac{\rho c U}{a\kappa_0 b^m}\right\}^{1/(1+m)} r^{-1/(1+m)}\tilde{i},\\ g &= \frac{a}{c}\left\{\frac{\rho c U}{a\kappa_0 b^m}\right\}^{2/(1+m)} r^{2m/(1+m)}\tilde{g},\\ s &= \rho U\left\{\frac{\rho c U}{a\kappa_0 b^m}\right\}^{1/(1+m)} r^{m/(1+m)}\tilde{s}.\end{aligned} \tag{10}$$

Comparing (4) and (10) shows the following correspondences:

$$\begin{aligned}&\left\{\frac{2m}{1+m}\right\}^{1/(1+m)}\Gamma(0) \Longleftrightarrow \tilde{i}(0),\\ &\left\{\frac{2m}{1+m}\right\}^{(1-m)/(1+m)}G(0) \Longleftrightarrow \tilde{g}(0),\\ &\left\{\frac{2m}{1+m}\right\}^{1/(1+m)}S(0) \Longleftrightarrow \tilde{s}(0).\end{aligned} \tag{11}$$

For either scaling the constitutive law takes the same form, i.e., $S = G\Gamma^m$ or $\tilde{s} = \tilde{g}\tilde{i}^m$. The advantage of the scaling in (4) is that $\Gamma(0) = 1$ in all cases, so that $G(0) = S(0) = S_0$. The relations among $\tilde{s}(0)$, $\tilde{g}(0)$, and $\tilde{i}(0)$ are not as simple, as seen from (11). The same manipulations that previously lead to (7) now lead to

$$U = \sqrt{\frac{s^+}{\rho}}\sqrt{\frac{-s_\theta^+}{\rho c}}\frac{\sqrt{\tilde{g}^+}}{\tilde{s}^+} \tag{12}$$

with Chen and Batra's equations. Now from (11) $\sqrt{\tilde{g}^+}/\tilde{s}^+ = \sqrt{(1+m)/2m}S_0^{-1/2}$ when the constitutive equations are scaled in the mode III form. Thus, the speed in either mode II or mode III is given by Eq. (7).

Furthermore, it may be checked from the equations in Chen and Batra (1999) that an equation entirely equivalent to (9) also holds for mode II motion.

3. Discussion

The speed of a shear band, according to Eq. (7), depends on the state of the material directly ahead of the tip of the fully localized band. The first term is a plastic wave speed, which is determined by the square root of the specific flow stress. This fundamental speed is modified by the square root of the rate of softening per unit plastic work. Stronger softening accelerates the band and weaker softening retards it. This observation tends to confirm the speculative remark of Bonnet-LeBouvier et al. (2002) quoted at the end of the first section. The speed is further modified by the inverse square root of the strain rate sensitivity so that stronger sensitivity retards the band and weaker sensitivity accelerates it. As always happens in shear band problems, the non-dimensional softening and the strain rate sensitivity do not appear individually, but as a ratio. Finally, note that the speed is not fully determined by material properties, but also requires the specification of the constant S_0, which plays the role of an initial value in determining the similarity solution. It would appear that the constant cannot be determined without reference to the complete boundary value problem of which the similarity solution is only one part. Further research is required to determine exactly how the constant is to be determined in any particular problem.

The author had previously conjectured that if the constitutive law for plastic flow were calibrated to the material directly in front of the band, then the undetermined constant must be 1.0, Wright (2002), but upon closer examination this does not appear to be the case. All attempts to establish such a procedure using only the similarity forms in Eq. (4) have resulted only in confirming the apparent arbitrariness of the constant without further information.

Eqs. (7) and (9) may be applied to the flow law in (1) with $n = 0$ and compared to the results of Bonnet-LeBouvier et al. (2002) in Eqs. (3) and (2) respectively. Because the relation between the flow stresses for tension and shear is $\sigma_e = \sqrt{3}s$, and because $-s_\theta = \nu s/T$ in this case, the results are

$$U = \frac{\sigma_e^+}{\sqrt{3}\rho}\sqrt{\frac{\nu}{cT^+}}\sqrt{\frac{1+m}{2m}}\frac{1}{\sqrt{S_0}} \quad \text{and} \quad \frac{U}{[w^-]/2} = \frac{1}{W^-}\frac{1+m}{2m}\frac{\nu\sigma_e^+}{\sqrt{3}\rho c T^+}. \tag{13}$$

As before, the superscript plus sign indicates that the quantity is to be evaluated directly ahead of the propagating tip of the shear band. For the narrow strip studied by Bonnet-LeBouvier et al. (2002) the driving velocity at the upper and lower boundaries, V, may be interpreted as $[w^-]/2$ until inertial effects start to become important in establishing the fields behind the point of localization. All the main features of Eqs. (3) and (2) are also captured by the two theoretical formulas given in Eq. (13) except for the dependence on work hardening.

Setting $S_0 = 1$ in Eq. (7) delivers a formula for the basic characteristic scale of the speed of a shear band. Although it will not deliver precise answers for particular boundary value problems, evaluation of the resulting formula for different materials will allow comparative predictions of the characteristic speeds of shear bands in those materials. However, such a comparison is strongly dependent on the constitutive model used for the flow stress. In turn this requires an abundance of high quality data, which is not always available. The weakest links tend to be the rate of thermal softening under high rate heating and the smaller values of strain rate sensitivity ($m < 0.01$, say). Rapid heating is important so that slower metallurgical changes, which are unimportant for adiabatic shear bands, will tend to be suppressed. Eqs. (7) and (9) are obviously extremely sensitive to small values of strain rate sensitivity, m, which are also the most difficult to establish experimentally with accuracy.

Table 1
Properties and characteristic speeds of an adiabatic shear band in various materials

Material	Flow stress (MPa)	Density (kg/m^3)	Specific heat (J/kg K)	Melting temperature (K)	$\sqrt{s/\rho}$ (m/s)	Thermal sensitivity ($-s_\theta/\rho c$)	Strain rate sensitivity (m)	Susceptibility ($-s_\theta/m\rho c$)	ASB speed (m/s)
2024-T351 Aluminum, B-75	280	2770	875	775	320	0.24	0.015	16	910
7039 Aluminum, B-76	280	2770	875	877	320	0.20	0.01	20	1000
1006 Steel, F-94	300	7890	452	1811	195	0.055	0.022	2.5	220
4340 Steel, C-30	660	7830	477	1793	290	0.12	0.014	9	600
S7 Tool steel, C-50	1150	7750	477	1763	385	0.21	0.012	18	1150
W–7Ni–3Fe, C-47	1060	17000	134	1723	250	0.33	0.016	21	800
U–3/4Ti, C-45	990	18600	117	1473	230	0.38	0.007	54	1210

Data adapted from Johnson and Cook (1983).

For example, Table 1 compares two aluminum alloys, three steels, a tungsten metal matrix composite, and a uranium alloy. The Johnson–Cook model of viscoplasticity has been used (Johnson and Cook, 1983) to estimate the flow stress, and all data have been taken from the same paper. Linear softening from room temperature (293 K) to the melting point has been assumed in every case in the absence of more robust data. The flow stress was calculated by arbitrarily assuming an equivalent plastic shear strain of 0.10 and an equivalent shearing strain rate of about 5200 s^{-1}. Since the formulas given in the paper are for equivalent tensile stress and strain, the assumed shear values must be converted to the appropriate tensile values and then the resulting tensile stress must be converted back to an equivalent shear value for use in Eq. (7). The strain rate sensitivity, m, is taken to be the constant C in their viscoplasticity model. This is a good approximation for small sensitivities, $m \ll 1$. The data and speeds given in the table cannot be regarded as precise, for reasons stated previously, but the table does illustrate how various physical properties can be expected to affect the speed of an adiabatic shear band.

The first column in the table lists the material and a nominal hardness on one of the Rockwell scales. The next four columns and the eighth column are adapted from Johnson and Cook (1983), as described above. The characteristic speed determined from the specific flow stress is given in the sixth column. The thermal sensitivity is estimated in the seventh column by taking $-s_\theta^+ = s^+/(T_{\text{melt}} - T_{\text{room}})$. The column labeled susceptibility is the ratio of the thermal and strain rate sensitivities. For a given non-dimensionalized defect the material with the greatest susceptibility may be expected to fail at the lowest shear strain in a torsional Kolsky bar test, Wright (1990). Finally the last column is the characteristic speed of an adiabatic shear band, as estimated by Eq. (7) and the available data.

The two aluminums have high characteristic speeds because even though the flow stresses are not high, the density is low. The low melting temperatures offset the large specific heats and low flow stresses to produce moderate values of thermal sensitivity. Strain rate sensitivities are on the low side, so the net result is that the estimated speed of a shear band in the aluminum alloys is fairly high. The three steels illustrate the effects of increasing strength and decreasing strain rate sensitivity on susceptibility and shear band speed. Finally note that the two high density materials, which show moderately low characteristic speeds, as expected, both show large thermal sensitivities because of low specific heats and high strengths. However, only the uranium alloy shows a high speed for shear bands. This is a consequence of an extremely high susceptibility, which follows from the exceptionally low strain rate sensitivity.

The main point to be drawn from this discussion is that the speed of an adiabatic shear band depends on many physical factors, including strength, density, specific heat, melting temperature (or more accurately, rate of thermal softening), and strain rate sensitivity. As a final comment, note that Eq. (7) depends on the state of the material immediately ahead of the fully developed shear band, but to locate that point in any boundary value problem would still require accurate knowledge of incipient localization.

References

Bonnet-LeBouvier, A.-S., Molinari, A., Lipinski, P., 2002. Analysis of the propagation of adiabatic shear bands. International Journal of Solids and Structures 39, 4249–4269.

Chen, L., Batra, R.C., 1999. The asymptotic structure of a shear band in mode-II deformations. International Journal of Engineering Science 37, 895–919.

Gioia, G., Ortiz, M., 1996. The two-dimensional structure of dynamic boundary layers and shear bands in thermoviscoplastic solids. Journal of the Mechanics and Physics of Solids 44, 251–292.

Guduru, P.R., Rosakis, A.J., Ravichandran, G., 2001. Dynamic shear bands: an investigation using high speed optical and infrared diagnostics. Mechanics of Materials 33, 371–402.

Johnson, G.R., Cook, W.H., 1983. A constitutive model and data for metals subjected to large strains, high strain rates, and high temperatures. In: Proceedings of the 7th International Symposium on Ballistics. pp. 541–547.

Kalthoff, J.F., 2000. Modes of dynamic shear failure in solids. International Journal of Fracture 101, 1–31.

Needleman, A., Tvergaard, V., 1995. Analysis of a brittle–ductile transition under dynamic shear loading. International Journal of Solids and Structures 32, 2571–2590.

Wright, T.W., 1990. Approximate analysis for the formation of adiabatic shear bands. Journal of the Mechanics and Physics of Solids 38, 515–530.

Wright, T.W., 2002. The physics and mathematics of adiabatic shear bands. Cambridge University Press, Cambridge.

Wright, T.W., Walter, J.W., 1996. The asymptotic structure of an adiabatic shear band in antiplane motion. Journal of the Mechanics and Physics of Solids 44, 77–97.